npj | Climate and Atmospheric Science

www.nature.com/npjclimatsci

ARTICLE OPEN

Check for updates

Quantifying non-CO_2 contributions to remaining carbon budgets

Stuart Jenkins[1]✉, Michelle Cain[1,2], Pierre Friedlingstein[3,4], Nathan Gillett[5], Tristram Walsh[1] and Myles R. Allen[1,6]

The IPCC Special Report on 1.5 °C concluded that anthropogenic global warming is determined by cumulative anthropogenic CO_2 emissions and the non-CO_2 radiative forcing level in the decades prior to peak warming. We quantify this using CO_2-forcing-equivalent (CO_2-fe) emissions. We produce an observationally constrained estimate of the Transient Climate Response to cumulative carbon Emissions (TCRE), giving a 90% confidence interval of 0.26–0.78 °C/TtCO_2, implying a remaining total CO_2-fe budget from 2020 to 1.5 °C of 350–1040 GtCO_2-fe, where non-CO_2 forcing changes take up 50 to 300 GtCO_2-fe. Using a central non-CO_2 forcing estimate, the remaining CO_2 budgets are 640, 545, 455 GtCO_2 for a 33, 50 or 66% chance of limiting warming to 1.5 °C. We discuss the impact of GMST revisions and the contribution of non-CO_2 mitigation to remaining budgets, determining that reporting budgets in CO_2-fe for alternative definitions of GMST, displaying CO_2 and non-CO_2 contributions using a two-dimensional presentation, offers the most transparent approach.

npj Climate and Atmospheric Science (2021)4:47 ; https://doi.org/10.1038/s41612-021-00203-9

INTRODUCTION

The IPCC's Special Report on Global Warming of 1.5 °C[1] (SR1.5) concluded: 'Reaching and sustaining net zero global anthropogenic CO_2 emissions and declining net non-CO_2 radiative forcing would halt anthropogenic global warming on multi-decadal timescales. The maximum temperature reached is then determined by cumulative net global anthropogenic CO_2 emissions up to the time of net zero CO_2 emissions and the level of non-CO_2 radiative forcing prior to the time that maximum temperatures are reached.' This highlights the importance of future cumulative CO_2 emissions, often termed the 'remaining carbon budget'[2–5], together with the increasingly important role of non-CO_2 climate drivers as peak warming is approached. SR1.5 did not, however, give any further scenario-independent quantification of this statement, beyond noting that an increase of 1 W/m^2 of non-CO_2 radiative forcing and a cumulative emission of 1000 GtCO_2 'represent approximately equal effects on global mean surface temperature (GMST).' Here we provide this quantification.

The carbon budget framing is helpful because most warming to date has been caused by CO_2[6–8], and CO_2, of all major pollutants, has the most permanent impact on the climate system[8–10]. CO_2-induced warming is approximately proportional to the total quantity of CO_2 emitted over any multi-decade time interval, where the constant of proportionality is termed the Transient Climate Response to cumulative carbon Emissions, or TCRE[5,11]. There are, however, complications[1,2,9,12] in the use of TCRE to derive the remaining carbon budget, including the precise definition and estimated current level of global warming; committed warming due to past CO_2 emissions, or the zero emissions commitment (ZEC); possible contributions of Earth System Feedbacks to future warming; uncertainty in the estimated value of the TCRE; and the future contribution of non-CO_2 climate pollutants. Of these, the contribution of non-CO_2 pollutants is unique in that it depends on future policy decisions, not simply scientific uncertainty.

We focus here on carbon budgets corresponding to increases in GMST because this remains the index used to report observed increases in global temperatures[1,13,14], and hence may be used to determine when a temperature threshold is reached. Previous studies have suggested that changing sea-ice cover precludes the use of GMST in projections[15]. However, Fig. 3f of ref. [15] indicates the very limited impact of sea-ice retreat on GMST under ambitious mitigation scenarios, while under sustained warming the impact would correspond to a couple of years of warming at most. Therefore, changing sea-ice cover does not present any fundamental impediment to the use of GMST in projections. Further, while in earlier GMST products the ratio of GSAT to GMST has differed by several percent[16], recent updates to GMST datasets have largely accounted for these differences using statistical infilling of undersampled geographical regions.

Here, headline conclusions are communicated for a global temperature anomaly calculated from a four-dataset mean of these statistically infilled GMST products (similar to the approach taken in ref. [17]) to reduce the impact of any individual dataset, and to ensure that our conclusions are consistent with the estimates of the current level and rate of increase of human-induced global warming (see 3,13,17). Recent updates to these GMST datasets have revised the present decade's warming level up compared to earlier products. This presents a hazard for policymakers: using different indices to report observed warming (e.g. the reference period chosen in the Structured Expert Dialogue[14] informing the Paris Agreement) and to calculate carbon budgets[15] raises the possibility of the carbon budget being exhausted well before a temperature threshold is reached, potentially undermining confidence in the entire construct. Following SR1.5, we focus on budgets consistent with halting warming for a multi-decade period, acknowledging uncertainty in the level of positive or

[1]AOPP, Department. of Physics, University of Oxford, Oxford, UK. [2]Centre for Environmental and Agricultural Informatics, Cranfield University, Cranfield, United Kingdom. [3]College of Engineering, Mathematics and Physical Sciences, University of Exeter, Exeter EX4 4QF, UK. [4]Laboratoire de Meteorologie Dynamique, Institut Pierre-Simon Laplace, CNRS-ENS-UPMC-X, Departement de Geosciences, Ecole Normale Superieure, 24 rue Lhomond, 75005 Paris, France. [5]Canadian Centre for Climate Modelling and Analysis, Environment and Climate Change Canada, Victoria, BC, Canada. [6]Environmental Change Institute, School of Geography, University of Oxford, Oxford, UK. ✉email: stuart.jenkins@wadham.ox.ac.uk

negative emissions that may be required to maintain stable temperatures in the very long term thereafter[18]. This allows us to assume the ZEC is negligible and ignore long-term Earth system feedbacks. Most studies find the ZEC contributes at most a small amount to remaining warming under ambitious mitigation scenarios[10,19–21].

Most recent estimates of a remaining 'multi-gas' carbon budget rely on subtracting a distribution of warming responses to non-CO_2 sources from the target total warming and estimating a CO_2 budget for the remainder[1,2,22]. This approach relies on: (1) the careful treatment of covarying physical climate response uncertainty to both CO_2 and non-CO_2 contributions and (2) available scenarios from integrated assessment models (IAMs) representing a statistical distribution of possible futures. Guidelines on the use of scenarios in the SR1.5 database make clear they should not be treated as a statistical distribution[23], since they rely on prescriptive, often normative, decisions such that the choice of model has more impact than within-model uncertainties (we show this in Fig. 3). Scenarios representing the most ambitious temperature goals also depend on which IAM set-ups converge at all, an even more arbitrary and opaque constraint. Therefore, percentiles of available scenarios cannot be used to estimate the 'likely' non-CO_2 contribution to warming. Further, a predetermined quantity of non-CO_2 warming should not be subtracted from the total remaining warming without considering the accompanying impact of covarying physical climate uncertainty implicit in the choice of TCRE. Refs. [1,2,24] all remove a quantity of warming attributed to non-CO_2 pollutants independent of the sampled TCRE percentile. A more transparent treatment of non-CO_2 climate drivers uses CO_2-forcing-equivalent (CO_2-fe) emissions[25], meaning the CO_2 emissions time series that would give precisely the same impact on effective radiative forcing (ERF) and thence GMST. This is similar to the approach of ref. [26], although they use a single representative non-CO_2 forcing scenario. By doing this we can explicitly sample the physical climate response uncertainty for both CO_2 and non-CO_2 contributions identically, and more clearly separate scenario and physical response uncertainties in non-CO_2 contributions. We are therefore here assuming the climate response to effective non-CO_2 forcing is identical to the response to the same level and time-history as CO_2 forcing: while still an assumption, this is clearly preferable to assuming these responses are independent.

RESULTS

CO_2-forcing-equivalent emissions in mitigation scenarios

Originally proposed by Tom Wigley in 1998 under the name of a 'Forcing-Equivalent Index', CO_2-fe emissions[27] express an emissions time series of any climate pollutant in terms of the time series of CO_2 emissions that would have an identical impact on ERF, and hence GMST on all timescales. They are obtained by converting the ERF associated with that pollutant to a time series of change in CO_2-equivalent concentrations, and then computing the CO_2 emissions required to produce that CO_2 concentration perturbation using a carbon cycle model[25] (see Methods for a full explanation of the CO_2-fe methodology along with a simple formula which approximates the full calculation).

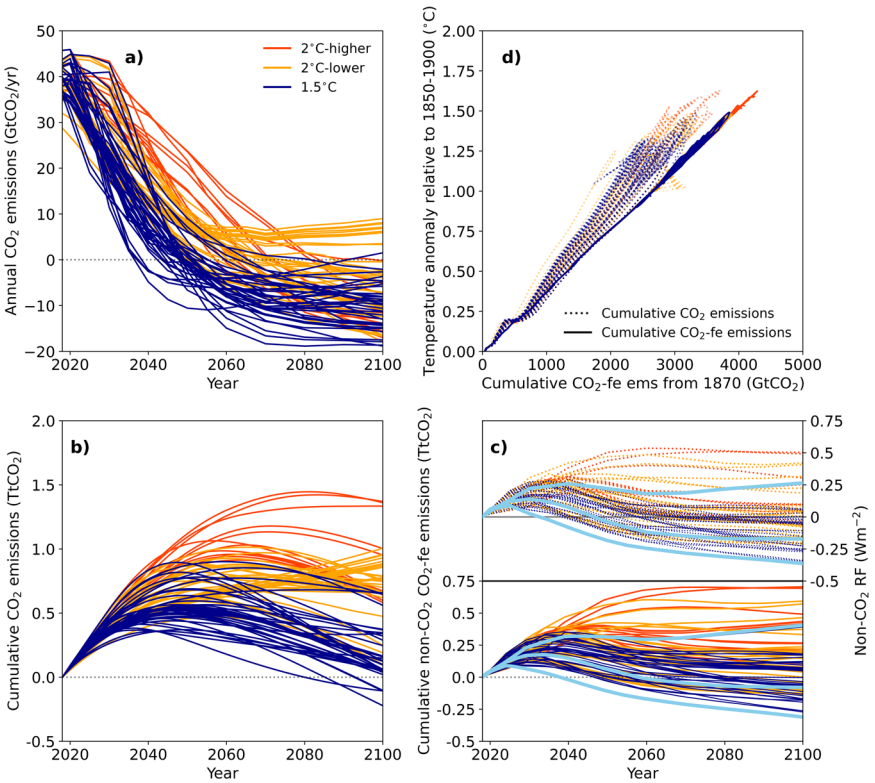

Fig. 1 IIASA IAMC database of scenarios in the IPCC Special Report on the Global Warming of 1.5 °C. Panel **a** plots the annual CO_2 emissions. Panel **b** (below **a**) shows the running sum (or cumulative) CO_2 emissions from 2018. Panel **c** (bottom right) shows the non-CO_2 radiative forcing for each scenario (dotted lines, right hand axis). Also on panel **c** are the cumulative non-CO_2 CO_2-fe emissions from 2018 corresponding to each non-CO_2 RF line (solid lines, left-hand axis). The axes of panels **b** and **c** are scaled so the cumulative emissions from CO_2 and non-CO_2 are directly comparable. Panel **d** plots the FaIRv2.0-derived temperature response against the diagnosed cumulative CO_2-fe emissions (solid lines) and against the cumulative CO_2-only emissions (dotted lines). For FaIR temperature response TCR = 1.8 °C, ECS = 3.0 °C. Scenarios are coloured by category in the IAMC database: red for 2 °C-higher, orange for 2 °C-lower and blue for 1.5 °C-compatible. Light blue scenarios in panel **c** highlight some example non-CO_2 pathways (lower bound, upper bound and a central scenario from 1.5 °C-compatible dark blue plume) with the central light blue scenario (P3 scenario from SR15 SPM.3b) also used in Figs. 2 and 3.

Removing a temperature contribution from non-CO_2 forcing agents would be a valid approach to carbon budget estimation so long as the physical climate response uncertainty were sampled at the same percentile for both CO_2 and non-CO_2 warming contributions. SR1.5, and similar approaches[2,24], remove a predetermined range of non-CO_2 warming before the TCRE is sampled. This is inconsistent since a low non-CO_2 warming contribution is significantly more likely if a low TCRE is sampled. A more transparent approach uses CO_2-fe: the scenario uncertainty (fraction of total CO_2-fe budget which is allocated to non-CO_2 forcing agents) is separated from the physical climate behaviour governing the overall size of the cumulative all-pollutant budget.

In contrast to conventional emission metrics, there is no need to specify an arbitrary time-horizon to compute CO_2-fe emissions, since the CO_2 emissions required to produce a particular pathway of concentration anomalies are unambiguously determined by the behaviour of the carbon cycle. IPCC's SR1.5 did not systematically include CO_2-fe in the estimation of remaining budgets[28] (it did address alternative metrics which approximate the behaviour of CO_2-fe, namely GWP*[29–31], but not in the analysis of carbon budgets). There is a clear need for complementary approaches, given that CO_2-fe is no less accurate than the temperature anomaly-based approach defined in SR1.5, and offers greater transparency since non-CO_2 forcing uncertainty is more clearly separated from physical climate uncertainty.

One benefit of the CO_2-fe metric is that it allows direct comparison between the CO_2 and non-CO_2 contributions to warming. In Fig. 1a we plot a number of scenarios for future CO_2 emissions from the IIASA SR1.5 scenario database[7]. They are coloured by ambition according to their label in the database; dark blue corresponds to scenarios tagged as '1.5 °C-compatible', light orange corresponds to 'lower-2 °C-compatible', and dark orange corresponds to 'higher-2 °C-compatible'. Panel b below shows the cumulative CO_2 emissions relative to 2018, which can be translated into the CO_2 warming contributions by multiplying by the TCRE. Panel c shows the corresponding non-CO_2 ERFs for each CO_2 emissions pathway (dotted lines, right axis). We would like to compare these scenarios to the CO_2 emissions, but we cannot simply apply the TCRE as we did for CO_2 as the total warming is non-linear when plotted against cumulative CO_2 emissions alone (dotted lines in panel d). If, instead, we express the non-CO_2 ERFs as cumulative CO_2-fe emissions, they are now physically equivalent quantities and the cumulative CO_2/CO_2-fe emissions time series in panels b and c (solid lines, left axis) can be directly compared. This would not be possible with CO_2-equivalent emissions calculated using the GWP or GTP metrics, which do not accurately reproduce the warming outcome for a complex multi-gas emissions pathway[29].

By converting the full range of pollutants into cumulative CO_2-fe emissions we can use the TCRE in the same way we did for CO_2 alone. Figure 1d shows global temperatures plotted against cumulative total CO_2-fe emissions (solid lines). Cumulative total CO_2-fe emissions multiplied by the TCRE predicts the temperature response, just as in a pure-CO_2 scenario. If non-CO_2 radiative forcing were correlated with cumulative CO_2 emissions in these scenarios, then the latter would also predict the response with a simple scaling factor, or 'effective TCRE', to account for a constant fractional contribution to warming from non-CO_2 drivers[3,32,33]. Figure 1d shows this is not always the case (nor is there any physical reason for it to be the case in complex multi-gas future scenarios)[34]: hence the impact of non-CO_2 forcing needs to be treated explicitly.

Having explained the utility of the CO_2-fe metric for assessing the relative CO_2 and non-CO_2 contributions to warming in mitigation scenarios, we now turn to a single scenario and explore the contributions from individual pollutants in greater detail. The three light blue scenarios in Fig. 1 display the range of non-CO_2 RF pathways exhibited in 1.5 °C-compatible scenarios, with the central light blue pathway highlighting the P3 scenario from SR1.5's SPM Fig. 3b[1] (middle of the road scenario which achieves 1.5 °C ambition). Figure 2 shows a breakdown of the total CO_2-fe emissions time series for this central light blue scenario in Fig. 1c. We extend back to pre-industrial using the historical RF time series from ref. [35], and calculate individual CO_2-fe emissions contributions using a differencing approach (see Methods). These individual contributions are stacked and coloured by pollutant, with the panel a showing the annual CO_2-fe emissions, and panel b showing the same cumulatively. In contrast to CO_2-equivalent emissions, whether computed with GWP_{100} or any other conventional metric, CO_2-fe emissions reflect the impact of individual climate drivers on global temperature (panel c), allowing them to be compared objectively. CO_2-fe provides a transparent and easily implementable approach which translates readily to warming: cumulative emissions contributions in panel 2b correspond to warming levels in panel 2c (we have used a TCRE of 0.4 °C/TtCO_2—our best-estimate TCRE found using

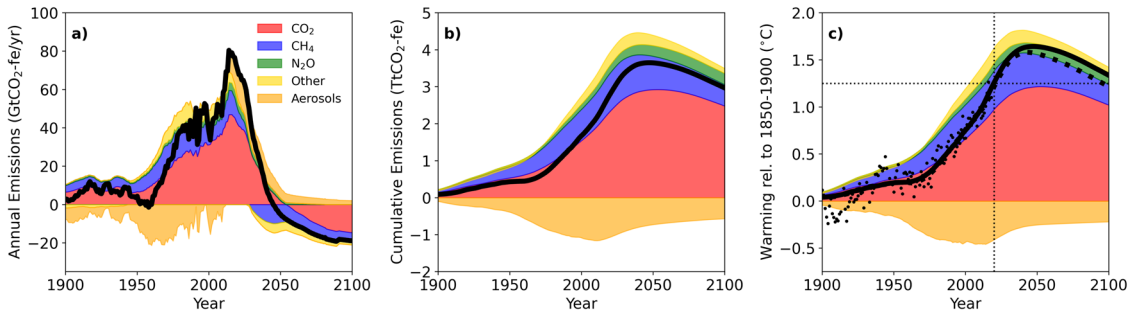

Fig. 2 Central light blue 1.5 °C-compatible scenario from Fig. 1 displayed showing component contributions to warming. Panel **a** plots the annual CO_2 emissions and CO_2-fe emissions for each of the major contributing pollutants (red = CO_2, blue = CH_4 + Ozone + Strat. H_2O, green = N_2O, gold = Other and orange = Aerosols). Panel **b** shows the corresponding cumulative CO_2 and CO_2-fe emissions time series (stacked by contribution to total). Panel **c** plots the temperature response for each component. Black solid lines show the total annual (panel **a**) and cumulative (panels **b** and **c**) CO_2-fe emissions, while the total temperature response is shown with a black dotted line (all calculated from total RF). Small backscatter points on panel **c** show the annual temperature observations using four-dataset mean observations updated from SPM.1, SR1.5. FaIR-derived temperatures (panel **c**) use thermal parameters chosen to best emulate historical temperatures (TCR = 1.8 °C, ECS = 3.0 °C). RFs before 2020 are taken for individual components from Dessler and Forster (2018) RF dataset, with future component RF rescaled to match the component's best-estimate historical RF in 2020. Methane forcing is scaled by 1.65 to account for Ozone and stratospheric H_2O contributions, following refs. [40,30]. Aerosol forcing is ~−0.9 W/m^2 in 2011, consistent with recent observationally constrained estimates (e.g. Stevens et al., 2015; AR5, 2013). Thin dotted lines show present-day best-estimate anthropogenic warming level (1.23 °C in 2020).

an observationally constrained methodology described in section 3 below).

Methane emissions make a net positive contribution to annual CO_2-fe emissions until they begin to rapidly decline. Thereafter, the short atmospheric residence time of methane[30] means that falling methane emissions give a declining radiative forcing, equivalent to negative CO_2-fe emissions. Aerosol cumulative CO_2-fe emissions in Fig. 2b are negative, but show a sharp increase towards zero in the 2020s and 2030s, corresponding to a high associated CO_2-fe emissions rate (orange in Fig. 2a), and consequently a rapid removal of the cooling effect that aerosols have been contributing over history. Long-lived pollutants like nitrous oxide behave like CO_2. Note that the calculation of CO_2-fe emissions is not model specific: with a linear CO_2 impulse response (IR) function (as used for the calculation of GWPs) one can calculate CO_2-fe emissions with a simple matrix inversion and get very similar results (see Methods and ref. [36]). The accuracy of CO_2-fe emissions for representing the radiative forcing and therefore temperature impacts of long- and short-lived pollutants gives it clear advantages over GWP_{100} for presenting mitigation scenarios aimed at limiting global warming[29].

Total cumulative CO_2-fe emissions and total anthropogenic warming are approximately proportional to the combined warming impact of CO_2 and methane, as indicated by cumulative CO_2-plus-methane CO_2-fe emissions, up to the present-day (red and blue in Fig. 2b, c), but diverge rapidly over the coming decades as aerosol forcing declines (orange). Strikingly, this aerosol decline contributes almost as much to future warming as the remaining CO_2 emissions in this central 1.5 °C-compatible scenario (panel c), highlighting the importance of common and comparable presentations of all climate drivers. Aerosols are often not included in figures showing multi-gas emission scenarios[19] because of the lack of a nonarbitrary way of displaying them on a common axis. This problem is resolved by CO_2-fe. Individual contributions to CO_2-fe emissions from 2020 to the time of peak warming under this scenario are CO_2: 555 $GtCO_2$; methane: −65 $GtCO_2$-fe; nitrous oxide: 65 $GtCO_2$-fe; aerosols: 290 $GtCO_2$-fe; other forcings: −45 $GtCO_2$-fe; giving a total CO_2-fe budget of 800 $GtCO_2$-fe.

Observational constraints on the TCRE

Having demonstrated how the TCRE can be extended to multi-gas scenarios using CO_2-fe emissions, we now consider how CO_2-fe emissions can be used to investigate the TCRE itself. Previous TCRE estimates[37] have compared cumulative pure-CO_2 emissions with warming attributable to CO_2 alone, but the fractional uncertainty in the latter is higher than uncertainty in total anthropogenic warming. Comparing total anthropogenic warming with total cumulative CO_2-fe emissions over the historical record presents a useful complementary approach.

To estimate anthropogenic warming over the historical period, we use conventional 'optimal fingerprinting' applied to GMST, as is defined in Haustein et al. (2017)[38]. This uses a two-timescale IR model[9,39,40] to estimate temperature responses to anthropogenic and natural forcing (for which we use a 1000-member ensemble of representative ERF time series[35]). A four-dataset mean GMST observation time series is then regressed onto each pair of natural and anthropogenic temperature response time series to determine the most likely contribution from each component, with added CMIP6 PIControl simulations included in the regression to account for internal climate variability. For a full discussion see Methods. Estimated anthropogenic warming in 2020 relative to 1850–1900 is 1.23 °C (1.06–1.42 °C) (5–95% confidence interval), higher than ref. [1] (SR1.5) due to updates in the datasets.

We express the 1000 anthropogenic ERF time series as CO_2-fe emissions pathways[25] accounting for uncertainty in cumulative CO_2 airborne fraction to date (0.4 ± 0.04[41]) in carbon cycle parameters. Dots in Fig. 3a show estimates of the total anthropogenic warming and cumulative all-pollutant CO_2-fe emissions, coloured by decade. For example, pink dots in Fig. 3a sample the resulting joint distribution of cumulative anthropogenic CO_2-fe emissions 1875 to 2015 inclusive and human-induced warming to the decade 2011–2020 relative to 1850–1900.

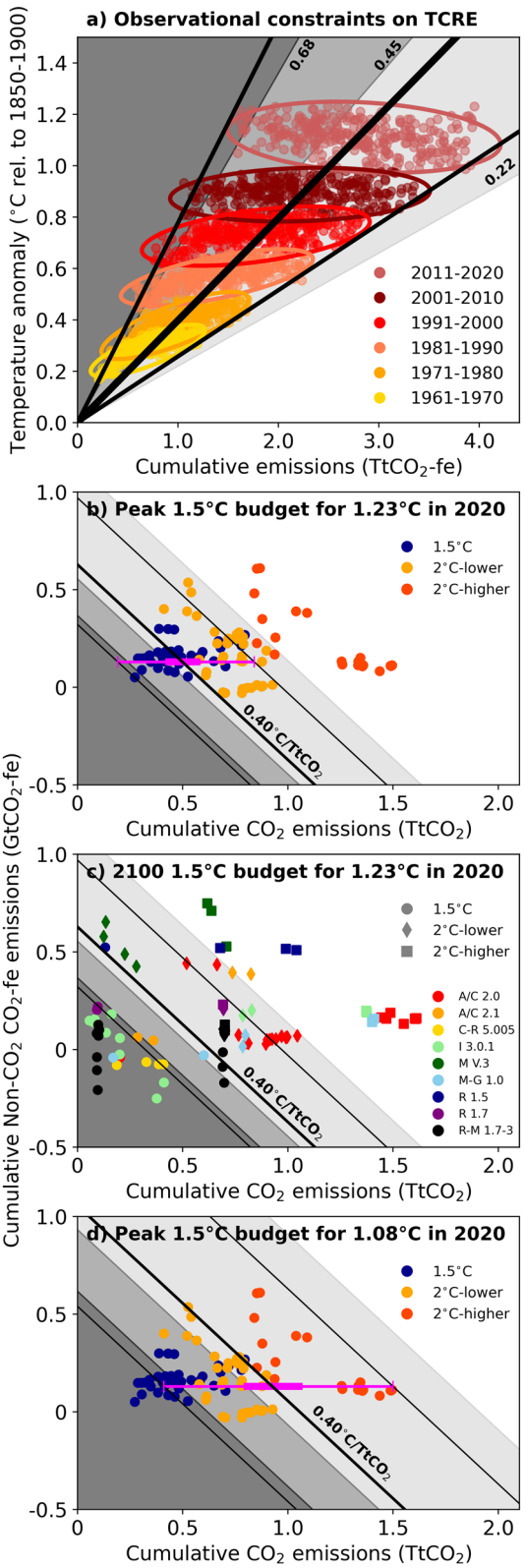

Fig. 3 Observational constraints on the TCRE and consequences for the design of Paris Agreement-compatible scenarios. Panel **a** plots attributed human-induced warming against cumulative emissions of CO_2. The space is shaded by the value of the TCRE (Gaussian distribution in best-estimate and likely range in AR5) and the points are coloured by the decade in which the temperature (relative to 1850–1900 baseline) and cumulative CO_2-fe emissions (relative to 1875) are diagnosed. An ellipse is drawn around central 90% of points. Black lines in panel **a** depict the 5th, 50th and 95th percentile of the overall observationally constrained TCRE distribution based on the 2011–2020 decade. Panels **b**–**d** show the remaining CO_2 and non-CO_2 CO_2-fe budgets from 2020 for each scenario in Fig. 1, coloured by category in the IIASA SR15 database. Panels **b** and **d** show remaining budgets to peak warming in each scenario, while panel **c** shows budgets to 2100 (instead coloured by IAM). In all three panels shading shows budgets compatible with limiting warming to 1.5 °C for the AR5 gaussian TCRE likely range, as in panel **a**. The solid black lines show the corresponding remaining total CO_2-fe budgets instead of using our observationally constrained TCRE 5th–95th percentile range. In panels **b** and **c** the shading, therefore, corresponds to budgets for 0.27 °C remaining warming to 1.5 °C-consistent with 1.23 °C warming in 2020. In panel **d** the shading refers to budget for 0.42 °C remaining warming to 1.5 °C-consistent with 1.08 °C warming in 2020 (re-baselining historical GMST to 0.85 °C for the decade prior to 2015). Pink horizontal box-whisker plots in panels **b** and **d** show estimates of remaining CO_2 budgets for each assumed present-day warming level, assuming a mid-range non-CO_2 budget to peak warming (130 $GtCO_2$-fe) and plotting the 5th, 33rd, 66th and 95th percentiles (see Methods for information on calculation). In panel **c** IAM abbreviations correspond to: A/C 2.0/2.1 – AIM/CGE 2.0/2.1; C-R 5.005 – C-Roads 5.005; I 3.0.1 – IMAGE 3.0.1; M V.3 – MESSAGE V.3; M-G 1.0 – MESSAGE-GLOBIOM 1.0; R 1.5/1.7 – REMIND 1.5/1.7; R-M 1.7-3 – REMIND-MAgPIE 1.7–3.0.

The cumulative anthropogenic CO_2-fe emissions and human-induced warming estimate for each dot correspond to the same ERF time series to account for any covariance, while CO_2 airborne fraction and internal climate variability are sampled independently. Shading shows the AR5 gaussian TCRE distribution, with the likely range and median values highlighted. Ellipses are drawn around each decade's scatter of covarying temperature anomaly and cumulative CO_2-fe emissions, encompassing the central 90% of the distribution, also coloured by decade. The best-fit TCRE is estimated as 0.40 °C/$TtCO_2$ (0.26–0.78 °C/$TtCO_2$ 90% confidence interval based on the most recent decade), marked with black lines in panel a. These could be interpreted as median and 5–95% percentiles of a probability distribution if the input ERF pathways are assumed to be equiprobable, but more research characterising the distribution of uncertainty in radiative forcing to date is needed[42].

For comparison, SR1.5 uses a likely TCRE range of 0.22–0.68 °C/$TtCO_2$ taken from the assessment in AR5's WG1 (SR1.5 also includes a 100–200 $GtCO_2$ budget correction accounting for differences between gaussian and log-normal TCRE distributions), while TCREs derived from the CMIP6 1%/yr CO_2 concentration increase experiment lie in the range 0.36–0.63 °C/$TtCO_2$ (see supplementary fig. 8, or ref. [43]). Other groups have separately diagnosed these (e.g. Williams et al.[44]), noting additionally that the inter-model spread is strongly affected by cloud feedbacks, particularly in high sensitivity models. Mengis and Matthews (2020) use the CO_2-fe metric to demonstrate the bias introduced by assuming a constant fractional non-CO_2 contribution to warming in TCRE assessments and estimate the TCRE using a single warming pathway (~0.5 °C/$TtCO_2$)[34]. Matthews et al. (2021) estimate an observationally constrained TCRE by removing a fractional warming contribution attributed to non-CO_2 pollutants, finding a median TCRE of 0.44 °C/$TtCO_2$ (0.32–0.62 °C/$TtCO_2$ 5–95th percentile range)[45]. We argue the contribution from

Table 1. TCRE percentiles and corresponding remaining carbon budgets to 1.5 °C.

Percentile	TCRE (GMST) (°C/$TtCO_2$)	1.5 °C remaining CO_2-fe budget ($TtCO_2$) (0.27 °C)	1.5 °C remaining CO_2-fe budget ($TtCO_2$) (0.42 °C)	1.5 °C remaining CO_2 budget ($TtCO_2$) (0.27 °C) 130 (50–300) $GtCO_2$-fe non-CO_2 budget	1.5 °C remaining CO_2 budget ($TtCO_2$) (0.42 °C) 130 (50–300) $GtCO_2$-fe non-CO_2 budget	SR1.5 1.5 °C remaining CO_2 budget ($TtCO_2$) (GMST)	SR1.5 1.5 °C remaining CO_2 budget ($TtCO_2$) (GSAT)	Rogelj et al (2019) 1.5 °C remaining CO_2 budget ($TtCO_2$) (GSAT)
5th	0.26	1.04	1.62	0.91 (0.74–0.99)	1.49 (1.32–1.57)	–	–	–
17th	0.31	0.87	1.35	0.74 (0.57–0.82)	1.22 (1.05–1.30)	-	–	–
33th	0.35	0.77	1.20	0.64 (0.47–0.72)	1.07 (0.90–1.15)	1.08	0.84	0.74
50th	0.40	0.68	1.06	0.55 (0.38–0.63)	0.93 (0.76–1.01)	0.77	0.58	0.48
66th	0.46	0.59	0.92	0.46 (0.29–0.54)	0.79 (0.62–0.87)	0.57	0.42	0.32
83th	0.57	0.47	0.73	0.34 (0.17–0.42)	0.60 (0.43–0.68)	–	–	–
95th	0.78	0.35	0.54	0.22 (0.05–0.30)	0.41 (0.24–0.49)	–	–	–

Percentiles of the TCRE found in this study are shown in column 2. CO_2-fe budgets for 0.27 °C additional warming (1.5 °C-compatible using GMST) and 0.42 °C additional warming (1.5 °C-compatible using GMST re-baselined to 0.85 °C over the decade up to 2015) shown in columns 3 and 4, respectively. Corresponding CO_2-only budgets to 1.5 °C are shown in columns 5 and 6, with mid-range non-CO_2 contribution (range shown in brackets for a full range of 1.5-compatible non-CO_2 contributions). For comparison, the headline remaining budget estimates in SR1.5 and Rogelj et al. (2019) are shown in columns 7, 8 and 9.

non-CO_2 pollutants should be determined explicitly using the CO_2-fe methodology.

The remaining total CO_2-fe emissions budgets for an additional 0.27 °C warming above 2020, corresponding to total warming of 1.5 °C, range between 350–1040 $GtCO_2$-fe. A detailed breakdown by percentile are shown in Table 1 (see Supplementary Table 1 for equivalent budgets to 2 °C). We calculate the remaining budgets for additional anthropogenic warming relative to the best-estimate current level (1.23 °C) for consistency with Table 2.2 of ref. [1], reflecting a policy focus on future warming relative to the recent past rather than including uncertainty in pre-industrial temperatures. The wide range of remaining total CO_2-fe budgets we find here are largely a result of the range of present-day RF in our 1000-member total anthropogenic RF ensemble. Reducing RF component uncertainty and accounting for correlations between component RFs would better constrain this range, and is a focus for future research. Here we focus on defining the methodology to estimate the TCRE with CO_2-fe.

Given these total remaining CO_2-fe budgets, the question now becomes what fraction of this budget is used by CO_2 and non-CO_2 pollutants respectively. Figure 3b shows the proportions of the future total CO_2-fe budget allocated to CO_2 and non-CO_2 in these scenarios. Shading indicates the remaining total budget compatible with 0.27 °C additional warming, again using the gaussian TCRE distribution reported in AR5 as in panel a, while solid black lines indicate the total remaining budget using our observationally constrained TCRE distribution from panel a. Scatter points indicate cumulative CO_2 and non-CO_2 CO_2-fe emissions to peak warming in 1.5 °C-compatible, 2 °C-lower and 2 °C-higher scenarios from Fig. 1, with the colours indicating the scenario category as in Fig. 1. In these scenarios, the non-CO_2 contribution to the total remaining budget ranges from 50–300 $GtCO_2$-fe, exactly the range determined in SR1.5 (where 250 $GtCO_2$ budget uncertainty was attributed to non-CO_2 scenario uncertainty). Depending on the TCRE, this means non-CO_2 scenario uncertainty contributes between 0.01 and 0.23 °C warming in these scenarios (using the observationally constrained TCRE 5th–95th percentile range). Importantly, dark blue 1.5 °C-compatible scenarios are consistent with their 1.5 °C peak warming categorisation—the scatter of blue dots sits over our best-estimate TCRE.

While individual scenario's CO_2 and non-CO_2 contributions to peak warming are shown in Fig. 3b, panel c instead plots the scenario's budgets out to 2100. Scenario categories are less clear if the budget is based on end of century warming—scenario categorisation appears overly conservative if the remaining budget is allocated to 2100, with around half of the 1.5 °C-consistent scenarios lying outside the likely range. Net-negative CO_2 emissions and declining non-CO_2 radiative forcing after mid-century reduce the cumulative contributions from both CO_2 and non-CO_2 pollutants (see Fig. 1b, c).

Further, Fig. 3c shows how this non-CO_2 contribution is influenced by the IAM choice. Colours indicate the IAM used to generate each scenario, confirming this is not a random distribution (as is discussed above in section 1), while the evident lack of correlation between cumulative CO_2 and non-CO_2-fe emissions to peak warming undermines the use of an 'effective' (multi-gas) TCRE. Since CO_2 and non-CO_2 emissions are affected by different policies, it is potentially misleading to present them using a single index such as percentage aggregate CO_2-equivalent emission reductions by a given date[46]. A two-dimensional presentation, separating CO_2 and non-CO_2 contributions to warming (as in panels 3b, c and d here), is the minimum required to ensure both indicators are on track to achieve a temperature goal. The sum of cumulative CO_2 and non-CO_2 CO_2-fe emissions, multiplied by the TCRE, determines long-term warming.

The scenarios explored here do not represent a random distribution that can be sampled for a particular percentile, so accounting for non-CO_2 contributions to remaining CO_2-only budget estimates is more challenging. Subtracting a representative mid-range scenario's non-CO_2 contribution from estimated total CO_2-fe budgets gives indicative pure-CO_2 budgets, indicated by horizontal box-whisker symbols in pink on Fig. 3 (using the central non-CO_2 RF scenario highlighted in Fig. 1). The range of non-CO_2 contributions implied by the non-CO_2 forcing scenarios as a whole indicates the potential for trade-offs between CO_2 and non-CO_2 warming.

Using GMST warming of 1.23 °C in 2020 and the mid-range non-CO_2 forcing from Fig. 1 (130 $GtCO_2$-fe), we find, for a 33, 50 and 66% chance of limiting warming to below 1.5 °C, indicative CO_2-only budgets of 640, 545, 455 $GtCO_2$ respectively. We re-emphasise this is just one possible pathway for future non-CO_2 forcing, which will be determined by policy choices, some but not all of which also involve trade-offs and synergies with CO_2 policy. Exploring these trade-offs is a matter for policymakers. CO_2-fe emissions, or warming-equivalent emissions[30] that are very similar and easier to calculate (see Methods), provide the necessary framework. SR1.5 gave 33rd, 50th and 66th percentile remaining carbon budgets for 1.5 °C GMST warming from 2018 of 1080, 770, 570 $GtCO_2$, respectively. Our best-estimate remaining carbon budget for 1.5 °C from 2020, 545 $GtCO_2$, is therefore consistent with SR1.5 having accounted for recent updates to the level of GMST and an additional 2 years of warming. SR1.5's GSAT best-estimate remaining carbon budget from 2018 is also consistent, albeit slightly more conservative (50th percentile remaining GSAT budget to 1.5 °C is 580 $GtCO_2$ from 2018) confirming that the infilled GMST products approximately correspond to GSAT remaining CO_2 budgets from the present-day. Our range of estimated remaining CO_2-only budgets are given in Table 1, along with comparable budgets from SR1.5.

The definition of present-day anthropogenic warming plays a key role in determining the size of remaining budgets, and therefore in determining the appropriate categories for scenarios. However, re-baselining anthropogenic warming to be consistent with the assessment that 0.85 °C warming occurred up to the 2006–2015 decade relative to 1850–1900 (a statement which is used in the Structured Expert Dialogue to inform the Paris Agreement text[14], and cited explicitly in discussions of 1.5 and 2.0 °C in the Paris Agreement by those familiar with the process[47]) results in a best-estimate remaining CO_2 budget from 2020 of 920 $GtCO_2$. Figure 3d shows that, then, scenarios currently classified as 'lower-2 °C' are consistent with a peak warming of ~1.5 °C. While revised estimates of present-day GMST used in Fig. 3b mean remaining carbon budgets are consistent with those presented in SR1.5, other interpretations of temperature levels referred to in the Paris Agreement, possibly more consistent with the consensus on the current level of warming at the time the Agreement was signed, may result in significantly larger remaining budgets.

Figure 3b, c, d together show that the current classification of the IAM scenarios are much more consistent with peak warming defined by the increase in statistically infilled (i.e. GSAT-like) GMST datasets relative to pre-industrial levels. Defining temperature this way also restores consistency with most other studies of remaining budgets (see Supplementary Tables 1, 2 of ref. [2]), at the expense of consistency with reported present-day levels of warming associated with recent impacts[14], although more closely aligning them with model-based studies of future impacts using GSAT[18].

To complement the assessment of TCREs using observations of the climate system, the TCREs for a subset of CMIP6 GCMs can be calculated over history directly using CO_2-fe emissions to account for the impact of non-CO_2 pollutants. Leach et al. (2020) demonstrate the FaIRv2.0[48] model can emulate the thermal and carbon cycle properties of CMIP6 GCMs, and provide fitted parameters for several CMIP6 models. RFMIP experiments[49] allow for the calculation of ERF time series over history (UKESM1-0-LL, NorESM2-LM, GFDL-ESM4) and extended up to 2100 where data is

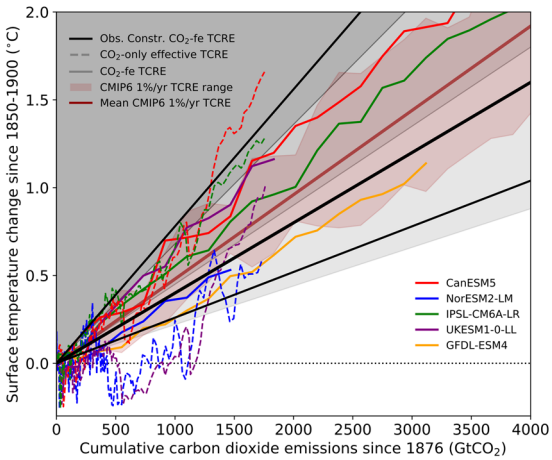

Fig. 4 TCREs calculated for a range of CMIP6 models. FaIRv2.0 simple climate model used to emulate the carbon cycle and thermal responses of each GCM with parameters from Leach et al. (2021); forced with ERF time series diagnosed from ERF experiments completed as part of RFMIP. UKESM1-0-LL and GFDL-ESM4 calculated GCM diagnosed aerosol ERF time series over 1850–2014; NorESM2-LM, IPSL-CM6A-LR and CanESM5 calculated using transient anthropogenic ERFs from RFMIP runs. Solid lines show individual CMIP6 model TCREs calculated with CO_2-fe over historical experiments (coloured by model), while dashed lines show CMIP6 models if the effective TCRE is plotted (1850–2014) from Lindicoat et al. (2021). Brown plume shows the CMIP6 TCRE range calculated with a 1%/yr concentration increase experiment (from Arora et al., 2020). Black shading shows the AR5 gaussian TCRE range, and black lines shows the observationally constrained TCRE range from Fig. 3.

available (CanESM5, IPSL-CM6A-LR). Using these, we diagnose the TCREs from estimates of the cumulative CO_2-fe emissions budgets and associated warming for each GCM, plotted in Fig. 4 (coloured solid lines; the full description in SI). If total warming is instead plotted against CO_2 emissions alone, nonlinearities are introduced (see Fig. 4, Supplementary Fig. 11, and dotted lines in Fig. 1d). For these five models, we find a CMIP6 TCRE range of 0.35–0.68 °C/$TtCO_2$, consistent with the range of observationally constrained GSMT TCRE from Fig. 3a (black lines in Fig. 4). CMIP6 ensemble members display TCREs which lie on average above the estimated 50th percentile of the observationally constrained distribution. Even UKESM1-0-LL and CanESM5, both of which have equilibrium climate sensitivities that are above the range consistent with historical observations[13,50] show high but not out-of-range TCRE estimates, lying around the 83rd percentile of the GMST TCRE distribution. These estimated TCREs can be compared with TCREs calculated using the 1%/yr CO_2 concentration increase experiment (brown plume in Fig. 4), and calculated in ref. [43]. CMIP6 TCREs estimated with CO_2-fe are near-identical to the estimates in Arora et al. (2020) using pure-CO_2, indicating the CO_2-fe methodology is indeed identifying the same TCRE parameter as in the 1%/yr idealised experiment. We present all calculated TCREs in supplementary table 2. The CMIP6 ensemble range appears to be consistent with the 5th–95th percentile TCRE found with historical observations, with extremes of the ensemble slightly under-sampling the observationally constrained upper and lower bounds. The mean response (0.48 °C/$TtCO_2$ in CMIP6 models assessed) is also somewhat higher than the observationally constrained result (0.40 °C/$TtCO_2$). Simply using the CMIP6 range in isolation as an uncertainty interval, therefore, is potentially problematic, despite the range implying no significant bias. A better approach would use observations to constrain the CMIP6 ensemble TCRE range, such as the yes/no exclusion for models based on historical temperature gradient reconstruction as suggested in Tokarska et al.[24].

DISCUSSION

Here we analyse IAM mitigation scenarios informing the IPCC's SR1.5 report, deconstructing them to highlight the relative contributions from CO_2 and non-CO_2 pollutants (Figs. 1 and 2). CO_2-fe emissions provide a means to quantify non-CO_2 contributions to future scenarios, without relying on traditional metrics which do not translate readily into a corresponding warming response. Further, we demonstrate that a simple scaling factor, or 'effective TCRE', doesn't adequately account for the warming contribution from non-CO_2 drivers[3,32,33] as future non-CO_2 radiative forcing isn't tightly correlated with cumulative CO_2 emissions in these scenarios. We also use CO_2-fe emissions to constrain the TCRE distribution based on historical temperature observations and radiative forcing estimates, and produce an observationally constrained remaining carbon budget estimate based on central non-CO_2 RF estimates, along with highlighting the covarying uncertainty in the physical climate response to CO_2 and non-CO_2 pollutants. We recommend that a two-dimensional presentation, which separates CO_2 and non-CO_2 contributions to warming (Fig. 3b–d) is the most transparent approach when displaying the physical constraints of remaining budgets.

A remaining carbon budget for 1.5 °C of 420 $GtCO_2$ from 2018 (the most widely quoted 66th percentile SR1.5 GSAT budget) is consistent with a current level of warming of 1.23 °C (in 2020 relative to 1850–1900)[16], given an observationally constrained TCRE (0.40 °C/$TtCO_2$; 0.26–0.78 °C/$TtCO_2$), unless we experience a sudden increase in the TCRE or future non-CO_2 climate forcing above the upper end of the range in the SR1.5 1.5 °C-compatible scenarios (see Fig. 3b and Table 1; although recent updates to datasets of observed CH_4 and N_2O mixing ratios suggest these are tracking a path higher than most future scenarios suggest[51,52]).

Re-baselining the current level of warming to 0.85 °C in the decade prior to 2015, a figure (based solely on GMST) that was used to contextualise the observed impacts of climate change in the Structured Expert Dialogue used to inform the Paris Agreement[14,17], is inconsistent with SR1.5's remaining budget estimates, and means that scenarios conventionally referred to as 'Lower-2.0 °C-consistent' in the IIASA SR1.5 scenario database are in fact 1.5 °C-consistent (panel d). A similar misclassification occurs if CO_2 and non-CO_2 CO_2-fe budgets are considered up to 2100 across the SR1.5 scenarios (panel 3c).

The decision on what index will be used to determine when 1.5 °C is reached has substantial policy implications and hence should not be determined by scientists alone. As long as observed warming continues to be reported in terms of GMST, continuing to report remaining carbon budgets in terms of GMST baselined to several periods (for example, both 0.85 °C over the decade prior to 2015; 1850–1900 pre-industrial baseline) seems the simplest and least policy-prescriptive option available. Regardless, we propose CO_2-fe emissions are the most transparent method to analyse the relative contributions from individual pollutants to remaining warming, particularly in order to disentangle scenario from physical climate uncertainty.

METHODS

Calculating CO_2 forcing-equivalent emissions

CO_2-fe emissions time series are computed with a four-pool carbon cycle model[9,25,48] based closely on the IR model used for metrics calculations in AR5[8,53], but with a minor modification to allow state-dependent time-scales: for these ambitious mitigation scenarios, very similar results are obtained using the AR5 formula itself (see Supplementary Fig. 3). The similarity of the dotted and solid lines in Fig. 1c shows that, over these

scenarios and timescales, a 1 W/m^2 change in ERF is approximately equivalent to 1000 GtCO$_2$-fe, consistent with Fig. 8.29 of ref. [40].

To calculate CO$_2$-fe emissions we calculate the CO$_2$ concentration associated with a given pollutant's RF scenario:

$$C_{\mathrm{ref}+\Delta F}(t) = C_0 \exp\frac{(\ln(2)(F_{\mathrm{ref}}(t)+\Delta F(t)))}{F_{2x}},\ C_{\mathrm{ref}}(t) = C_0 \exp\left(\frac{\ln(2)F_{\mathrm{ref}}(t)}{F_{2x}}\right), \quad (1)$$

where F_{ref} (t) is the reference scenario's RF (i.e. the forcing due to all-pollutants other than the one we are considering), and ΔF (t) are the RF of the given pollutant. F_{2x} is the RF for successive doublings in CO$_2$ concentration.

Following this, we calculate the CO$_2$ emissions compatible with each concentration pathway $C_{\mathrm{ref}+\Delta F}(t)$ and $C_{\mathrm{ref}}(t)$:

$$\begin{aligned} &E_{\mathrm{ref}+\Delta F\,/\,\mathrm{ref}}(t) = C_{\mathrm{ref}+\Delta F\,/\,\mathrm{ref}}(t) - C_0 - \sum_{i=0}^{3} R_i(t-1)g_i; \\ &\quad \text{with } R_i(t) = a_i E(t) + R_i(t-1)g_i\,; \\ &\quad\quad \text{and } g_i = \exp\left(\frac{-1}{a(t)\tau_i}\right), \end{aligned} \quad (2)$$

$$\Delta E(t) = E_{\mathrm{ref}+\Delta F}(t) - E_{\mathrm{ref}}(t), \quad (3)$$

where $E_{\mathrm{ref}+\Delta F}(t)$ and $E_{\mathrm{ref}}(t)$ are the annual emissions at time t resulting in concentrations $C_{\mathrm{ref}+\Delta F}(t)$ and $C_{\mathrm{ref}}(t)$. C_0 is the pre-industrial CO$_2$ concentration, a_i and τ_i are coefficients defined in the AR5 IR model and a (t) is a scaling factor on response timescales to allow for a changing airborne fraction over time, as detailed in ref. [3]. Finally, we find the CO$_2$-fe emissions attributable to pollutants with RF time series ΔF (t) by differencing the calculated annual emissions from the all forcing case, and the annual emissions for the case where we remove the RF from the pollutant: (ref + ΔF) − (ref).

Figures 1, 2, 3 and 4 all rely on CO$_2$-fe emissions calculated as above by inverting the carbon cycle of FaIR. A differencing approach is taken when calculating individual pollutant CO$_2$-fe emissions time series, as this is suggested in Jenkins et al. (2018) to best account for nonlinearities in the carbon cycle response to under high RF perturbations[25].

For ambitious mitigation scenarios, we can linearise the system to this calculation further. Now, a non-CO$_2$ ERF time series ΔF (t) due to a particular climate forcing agent is converted to a perturbation CO$_2$ concentration, accounting for the nonlinearity in CO$_2$ forcing, as follows:

$$\Delta C(t) = C_0 \exp\left(\frac{\ln(2)(F_{\mathrm{ref}}(t))}{F_{2x}}\right)\left(\exp\left(\frac{\ln(2)(\Delta F(t))}{F_{2x}}\right) - 1\right) \approx \frac{\Delta F(t)}{RE} \quad (4)$$

where F_{ref} (t) is the forcing due to all other agents, F_{2x} is the forcing due to a CO$_2$ doubling and C_0 is the pre-industrial CO$_2$ concentration, and RE is the radiative efficiency of CO$_2$ given present-day concentrations. The CO$_2$-fe emission time series is then found using the following iterative formula:

$$\begin{aligned} &\Delta E(t) = \Delta C(t) - \sum_{i=0}^{3} R_i(t-1)g_i\,; \\ &R_i(t) = a_i \Delta E(t) + R_i(t-1)g_i\,;\ \ g_i = \exp\left(\frac{-1}{a(t)\tau_i}\right) \end{aligned} \quad (5)$$

For ambitious mitigation scenarios, the linearization a (t) = 1 and constant RE provides a very close approximation to the full carbon cycle inversion. Setting a (t) = 1 in this way reproduces the linear IR model used in metric calculations of Chapter 8, AR5[40].

Approximating the CO$_2$-fe calculation

The calculation of CO$_2$-fe emissions in Figs. 1 and 2 does not require a specific model. In the main text, we invert the carbon cycle in the FaIRv1.0 simple climate model to calculate compatible CO$_2$-fe emissions with a given forcing input. In Supplementary Figs. 3 and 4 we reproduce these figures by calculating the CO$_2$-fe emissions with the AR5 IR model[2]. This model is also employed for metric calculations in IPCC's AR5. The AR5 model is linear, meaning it can be inverted as a matrix to calculate CO$_2$-fe emissions[54].

Converting all climate forcing agents to CO$_2$-fe emissions provides the most accurate and physically justified definition of an 'all-pollutants CO$_2$ budget' but requires full forcing histories and an invertible carbon cycle model. On decade-to-century timescales, however, CO$_2$-fe emissions associated with any individual forcing agent may be approximated by 'warming equivalent' emissions, CO$_2$-we, a linear combination of the components RF level and trend over a recent time interval, Δt.

First, considering how CO$_2$ emissions alone impact the global temperature anomaly. For CO$_2$ the change in radiative forcing, ΔFco$_2$, due to CO$_2$ emissions over an interval Δt depends on both the cumulative CO$_2$ emissions over that period, G, and the average-CO$_2$ induced forcing, $\overline{F_{\mathrm{CO2}}}$:

$$\Delta F_{\mathrm{CO2}} = \beta G - \rho \overline{F_{\mathrm{CO2}}} \Delta t \quad (6)$$

where the coefficient β is the additional radiative forcing per tonne CO$_2$ emitted (around 1 W/m^2 per 1000 GtCO$_2$), and ρ is the rate at CO$_2$-induced RF declines after CO$_2$ emissions reach zero. We can rearrange this formula to consider how to treat non-CO$_2$ radiative forcing contributions in terms of a cumulative CO$_2$-we budget, G_*:

$$G_* = \left(\Delta F + \rho \overline{F} \Delta t\right)/\beta \quad (7)$$

Therefore, to calculate the total human-induced warming associated with a CO$_2$ emissions time series, E(t), and a non-CO$_2$ forcing time series, F (t), over a time period Δt we can write:

$$\Delta T = \kappa(G + G_*) = \kappa\left(G + \frac{\Delta F}{\beta} + \frac{\rho \overline{F} \Delta t}{\beta}\right) \quad (8)$$

where the first term in brackets are the cumulative CO$_2$ emissions, the second is the CO$_2$ budget associated with a change in non-CO$_2$ RF ΔF, and the third is the CO$_2$ emissions budget associated with the average global energy imbalance due to non-CO$_2$ sources, $\overline{F}$. κ is the TCRE. Values of β and ρ can be related back to the AGWP$_{\mathrm{CO2}}$; typical values are β = 1 W/m^2 per 1000 GtCO$_2$, and ρ = 0.3% per year. The AR5 likely range for TCRE is 0.45 ± 0.23 °C per 1000 GtCO$_2$ (and in Fig. 3 we estimate a TCRE likely range between 0.26–0.78 °C/TtCO$_2$) which far outweighs uncertainty in other coefficients. The third term is relatively small in almost all scenarios but is retained to emphasise that halting warming due to non-CO$_2$ climate drivers requires declining, not constant, non-CO$_2$ forcing, although the required rate of decline is small: of the order of 1–3% per decade. For comparison of this formula with the full CO$_2$-fe calculation see Supplementary Fig. 2.

These options, along with simplifications such as GWP*, mean there are a number of alternatives to plotting the less physically representative GWP$_{100}$ emissions time series for non-CO$_2$ pollutants, even if in a given setting the full CO$_2$-fe calculation isn't appropriate.

Observationally constrained TCRE estimate

We estimate the TCRE in Fig. 3 using an observationally constrained methodology. We first estimate the present-day temperature anomaly, using an optimal fingerprinting approach outlined in Haustein et al. (2017)[38], and based on methodologies in refs. [55,56].

The approach uses ordinary least-squares (OLS) regression onto observed GMST to find the residual-minimising combination of anthropogenic and natural temperature responses. For GMST we use a four-dataset-mean of HadCRUT5 (statistically infilled)[57], NOAA[58], Berkeley[59] and GISTEMP[60], similar to Chapter 1, SR15[17]. The optimal fingerprinting methodology additionally samples uncertainty from internal variability (by sampling detrended CMIP6 PIControl experiment GSAT time series (104 members)[61]); along with a range of physical climate response parameters in the FaIR model when deriving temperature response shapes (18 members); uncertainty in the observed temperature anomaly using a 200-member ensemble of observational uncertainty from HadCRUT5. The derived present-day warming level (1.23 °C (1.06–1.42 °C) in 2020; 1.12 °C (0.90–1.33 °C) average over decade 2010–2019) is in agreement with other recent assessments of the present-day warming level (e.g. Gillett et al., 2021).

With this derived warming level, we now must determine the corresponding all-pollutant cumulative CO$_2$-fe emissions. We do this by inverting the FaIRv1.0 carbon cycle as derived above, with carbon cycle response parameters determine by best-estimate fits the historical relationship between carbon emissions and concentrations (from Jenkins et al., 2018), using historical temperature observations to inform likely historical carbon cycle temperature feedback behaviour. A 1000-member all-pollutant total anthropogenic ERF ensemble from ref. [35] is used to calculate a 1000-member ensemble of cumulative CO$_2$-fe emissions over history, which we plot against the decadal warming levels to produce Fig. 3a. Ellipses are drawn around the central 90% of the underlying decade scatterpoint distributions, using a similar approach to that used in Fig. 1 in ref. [62]. TCRE estimates are found based on the decade (2011–2020). The observationally constrained TCRE distribution has a log-normal shape and is plotted in Supplementary Fig. 6.

Defining remaining budgets to 1.5 °C

To define the remaining CO_2 budgets from present-day we must remove from the total CO_2-fe budget the contribution from non-CO_2 sources of warming. Using the highlighted scenarios in Fig. 1c we find compatible non-CO_2 contributions of between 50–300 $GtCO_2$ to peak warming in 1.5 °C-compatible scenarios in the IIASA SR15 database, with a central estimate of 130 $GtCO_2$.

The observationally constrained range of TCREs found in Fig. 3 of the main text is 0.26–0.78 °C/$TtCO_2$ (central 90 percent of distribution; 0.95–2.86 °C/TtC) with a best-estimate value of 0.40 °C/$TtCO_2$ (1.46 °C/TtC). Using the methodology of Haustein et al. (2017)[38] we find an estimated 2020 anthropogenic temperature anomaly = 1.23 °C, (5th–95th percentile = 1.06–1.42 °C) (see Supplementary Fig. 5d).

Therefore, the range of total CO_2-fe remaining budgets to 1.5 °C assuming best-estimate warming to date is:

Max: $(1.5–1.23) \times 1000/0.26 = 1040$ $GtCO_2$
Min: $(1.5–1.23) \times 1000/0.78 = 350$ $GtCO_2$
Best-estimate: $(1.5–1.23) \times 1000/0.40 = 680$ $GtCO_2$

Assuming a central estimate of the 1.5 °C-compatible non-CO_2 budget remaining from 2020 to peak warming (130 $GtCO_2$-fe in a central light blue scenario from Fig. 1, range 50–300 $GtCO_2$-fe) we find the remaining carbon budget to 1.5 °C corresponding to different TCRE percentiles as follows:

5th percentile: $(0.27 \times 1000/0.26) - 130 = 1040 - 130 = 910$ $GtCO_2$ (range: 740–990 $GtCO_2$)
33rd percentile: $(0.27 \times 1000/0.35) - 130 = 770 - 130 = 640$ $GtCO_2$ (range: 470–720 $GtCO_2$)
50th percentile: $(0.27 \times 1000/0.40) - 130 = 680 - 130 = 550$ $GtCO_2$ (range: 380–630 $GtCO_2$)
66th percentile: $(0.27 \times 1000/0.46) - 130 = 590 - 130 = 460$ $GtCO_2$ (range: 290–540 $GtCO_2$)
95th percentile: $(0.27 \times 1000/0.78) - 130 = 350 - 130 = 220$ $GtCO_2$ (range: 50–300 $GtCO_2$)

This methodology is followed to find remaining CO_2-fe budgets in Table 1 and to find CO_2-only budgets at the 33rd, 50th and 66th percentile in the main text and for pink error bars in Fig. 3b, d.

CO_2-fe breakdown of an example 1.5 °C-compatible scenario

Figure 2 uses the same best-estimate historical ERF from ref. [35] which is the basis for the observationally constrained TCRE in Fig. 3. Over the remainder of the 21st century (after 2020) we use the central non-CO_2 forcing scenario from Fig. 1c (highlighted in light blue). Components of ERF are rescaled to match 2020 ERF in the historical ERF time series. Aerosol ERF is consistent with -0.9 W/m^2 in 2011 (the value reported in Chapter 8, AR5; refs. [42,63]).

Component CO_2-fe budgets to peak warming are reported in the main text. Component 2100 budgets are: CO_2: 140 $GtCO_2$; methane: -455 $GtCO_2$-fe; nitrous oxide: 90 $GtCO_2$-fe; aerosols: 500 $GtCO_2$-fe; other forcings: -220 $GtCO_2$-fe; giving a total CO_2-fe budget of 55 $GtCO_2$-fe. Figure 2 reports a slightly different non-CO_2 cumulative CO_2-fe budget to peak warming than is used in Fig. 3. This is a result of scalings which are used in Fig. 2 to match IAM output to historical ERF estimates (the difference is equivalent to around a year of warming).

CMIP6 TCREs in Fig. 4

Figure 4 compares CMIP6 model TCREs to the observationally constrained distribution from Fig. 3. We use Arora et al. (2020)'s TCRE estimates using 1%/yr experiments, and compare to TCREs derived with a full CO_2-fe methodology where available historical ERF data is available from RFMIP[49]. Parameters derived using FaIRv2.0 to reproduce carbon cycle behaviour in individual CMIP6 models are given in Leach et al.[48]. We use these to estimate the TCRE for the five models [CanESM5, UKESM1-0-LL, IPSL-CM6A-LR, NorESM2-LM, GFDL-ESM4] where ERF data is available. These TCREs (reproduced for individual models in Supplementary Table 2) agree well with 1%/yr concentration increase TCRE estimates in Arora et al. (2020). Historcial CO_2 emissions from Lindicoat et al. (2020) are also used to show CO_2-only effective TCREs (dashed lines).

DATA AVAILABILITY

All data required to reproduce the figures in this paper are available freely online, and relevant databases and repositories are referenced in the text.

CODE AVAILABILITY

All codes required to reproduce the figures in this paper are available from the corresponding author.

Received: 19 January 2021; Accepted: 13 September 2021;
Published online: 14 October 2021

REFERENCES

1. IPCC. *Summary for Policymakers of the Special Report on the Global Warming of 1.5 °C* (IPCC, 2018).
2. Rogelj, J., Forster, P. M., Kriegler, E., Smith, C. J. & Séférian, R. Estimating and tracking the remaining carbon budget for stringent climate targets. *Nature* **571**, 335 (2019).
3. Leach, N. J. et al. Current level and rate of warming determine emissions budgets under ambitious mitigation. *Nat. Geosci.* **11**, 574 (2018).
4. Millar, R. J. et al. Emission budgets and pathways consistent with limiting warming to 1.5 °C. *Nat. Geosci.* **10**, 741–747 (2017).
5. Matthews, H. D., Gillett, N. P., Stott, P. A. & Zickfeld, K. The proportionality of global warming to cumulative carbon emissions. *Nature* **459**, 829–832 (2009).
6. Quere, C. L. et al. Global Carbon Budget 2018. *Earth Syst. Sci. Data* **10**, 2141–2194 (2018).
7. Huppmann, D. et al. *IAMC 1.5 °C Scenario Explorer and Data hosted by IIASA*. (Integrated Assessment Modeling Consortium & International Institute for Applied Systems Analysis, 2018). https://doi.org/10.22022/SR15/08-2018.15429
8. Joos, F. et al. Carbon dioxide and climate impulse response functions for the computation of greenhouse gas metrics: a multi-model analysis. *Atmos. Chem. Phys.* **13**, 2793–2825 (2013).
9. Millar, R. J., Nicholls, Z. R., Friedlingstein, P. & Allen, M. R. A modified impulse-response representation of the global near-surface air temperature and atmospheric concentration response to carbon dioxide emissions. *Atmos. Chem. Phys.* **17**, 7213–7228 (2017).
10. Ehlert, D. & Zickfeld, K. What determines the warming commitment after cessation of CO2 emissions? *Environ. Res. Lett.* **12**, 015002 (2017).
11. Allen, M. R. et al. Warming caused by cumulative carbon emissions towards the trillionth tonne. *Nature* **458**, 1163–1166 (2009).
12. Matthews, H. D., Zickfeld, K., Knutti, R. & Allen, M. R. Focus on cumulative emissions, global carbon budgets and the implications for climate mitigation targets. *Environ. Res. Lett.* **13**, 010201 (2018).
13. WMO. *WMO Provisional Statement on the State of the Global Climate in 2019* (WMO, 2019).
14. UNFCCC. *Report on the Structured Expert Dialogue on the 2013–2015 Review* (UNFCCC, 2015).
15. Tokarska, K. B. et al. Recommended temperature metrics for carbon budget estimates, model evaluation and climate policy. *Nat. Geosci.* **12**, 964–971 (2019).
16. Gillett, N. P. et al. Constraining human contributions to observed warming since the pre-industrial period. *Nat. Clim. Change* **11**, 1–6 (2021).
17. Allen, M. R. et al. Framing and Context. In: V, Masson-Delmott et al. (eds) *Global Warming of1.5°C. An IPCC Special Report on the impacts of global warming of 1.5°C above pre-industrial levels and related global greenhouse gas emission pathways, in the context of strengthening the global response to the threat of climate change, sustainable development, and efforts to eradicate poverty*. (2018).
18. Collins, M. et al. *Long-term Climate Change: Projections, Commitments and Irreversibility* (IPCC AR5, 2013).
19. Matthews, H. D. & Zickfeld, K. Climate response to zeroed emissions of greenhouse gases and aerosols. *Nat. Clim. Change* **2**, 338–341 (2012).
20. MacDougall, A. H. et al. Is there warming in the pipeline? A multi-model analysis of the zero emissions commitment from CO_2. *Biogeosciences* **17**, 2987–3016 (2020).
21. Jones, C. D. et al. The zero emissions commitment model intercomparison project (ZECMIP) contribution to C4MIP: quantifying committed climate changes following zero carbon emissions. *Geosci. Model Dev.* **12**, 4375–4385 (2019).
22. IPCC. *AR5 Synthesis Report: Climate Change 2014.* (IPCC, 2013). https://www.ipcc.ch/report/ar5/syr/.
23. Huppmann, D., Rogelj, J., Kriegler, E., Krey, V. & Riahi, K. A new scenario resource for integrated 1.5 °C research. *Nat. Clim. Change* **8**,1027–1030 (2018).
24. Tokarska, K. B. et al. Uncertainty in carbon budget estimates due to internal climate variability. *Environ. Res. Lett.* **15**, 104064 (2020).
25. Jenkins, S., Millar, R. J., Leach, N. & Allen, M. R. Framing climate goals in terms of cumulative CO2-forcing-equivalent emissions. *Geophys. Res. Lett.* **45**, 2795–2804 (2018).

26. Mengis, N., Partanen, A.-I., Jalbert, J. & Matthews, H. D. 1.5 °C carbon budget dependent on carbon cycle uncertainty and future non-CO 2 forcing. *Sci. Rep.* **8**, 1–7 (2018).
27. Wigley, T. M. L. The Kyoto Protocol: CO2 CH4 and climate implications. *Geophys. Res. Lett.* **25**, 2285–2288 (1998).
28. Forster, P. D. et al. *IPCC Special Report on the Global Warming of 1.5C* (IPCC, 2018).
29. Allen, M. R. et al. A solution to the misrepresentations of CO 2 -equivalent emissions of short-lived climate pollutants under ambitious mitigation. *Npj Clim. Atmos. Sci.* **1**, 16 (2018).
30. Cain, M. et al. Improved calculation of warming-equivalent emissions for short-lived climate pollutants. *Npj Clim. Atmos. Sci.* **2**, 1–7 (2019).
31. Lynch, J., Cain, M., Pierrehumbert, R. & Allen, M. Demonstrating GWP\ast: a means of reporting warming-equivalent emissions that captures the contrasting impacts of short- and long-lived climate pollutants. *Environ. Res. Lett.* **15**, 044023 (2020).
32. Matthews, H. D. et al. Estimating carbon budgets for ambitious climate targets. *Curr. Clim. Change Rep.* **3**, 69–77 (2017).
33. Millar, R. J. & Friedlingstein, P. The utility of the historical record for assessing the transient climate response to cumulative emissions. *Philos. Trans. R. Soc. Math. Phys. Eng. Sci.* **376**, 20160449 (2018).
34. Mengis, N. & Matthews, H. D. Non-CO 2 forcing changes will likely decrease the remaining carbon budget for 1.5 °C. *Npj Clim. Atmos. Sci.* **3**, 1–7 (2020).
35. Dessler, A. E. & Forster, P. M. An estimate of equilibrium climate sensitivity from interannual variability. *J. Geophys. Res. Atmos.* **123**, 8634–8645 (2018).
36. Allen, M., Jenkins, S., Sha, F. & Macey, A. Defining carbon neutrality, climate neutrality and net zero emissions. *Climate Policy* (2021, In Review).
37. Gillett, N. P., Arora, V. K., Matthews, D. & Allen, M. R. Constraining the ratio of global warming to cumulative CO2 emissions using CMIP5 simulations. *J. Clim.* **26**, 6844–6858 (2013).
38. Haustein, K. et al. A real-time global warming index. *Sci. Rep.* **7**, 15417 (2017).
39. Geoffroy, O. et al. Transient climate response in a two-layer energy-balance model. Part I: analytical solution and parameter calibration using CMIP5 AOGCM experiments. *J. Clim.* **26**, 1841–1857 (2012).
40. Myhre, G. et al. Anthropogenic and Natural Radiative Forcing. In: Stocker, T. F. et al. (eds) Climate Change 2013: The Physical Science Basis. Contribution of Working Group I to the Fifth Assessment Report of the Intergovernmental Panel on Climate Change. Cambridge University Press, Cambridge, United Kingdom and New York, NY, USA (2013).
41. Friedlingstein, P. et al. Global carbon budget 2019. *Earth Syst. Sci. Data* **11**, 1783–1838 (2019).
42. Bellouin, N. et al. Bounding global aerosol radiative forcing of climate change. *Rev. Geophys.* **58**, e2019RG000660 (2020).
43. Arora, V. K. et al. Carbon–concentration and carbon–climate feedbacks in CMIP6 models and their comparison to CMIP5 models. *Biogeosciences* **17**, 4173–4222 (2020).
44. Williams, R. G., Ceppi, P. & Katavouta, A. Controls of the transient climate response to emissions by physical feedbacks, heat uptake and carbon cycling. *Environ. Res. Lett.* **15**, 0940c1 (2020).
45. Damon Matthews, H. et al. An integrated approach to quantifying uncertainties in the remaining carbon budget. *Commun. Earth Environ.* **2**, 1–11 (2021).
46. United Nations Environment Programme (2019). Emissions Gap Report 2019. *UNEP, Nairobi.*
47. Mace, M. J. Mitigation commitments under the Paris Agreement and the Way Forward. *Clim. Law* **6**, 21–39 (2016).
48. Leach, N. J. et al. FaIRv2.0.0: a generalised impulse-response model for climate uncertainty and future scenario exploration. *Geosci. Model Dev.* **14**, 1–29 (2020).
49. Pincus, R., Forster, P. M. & Stevens, B. The radiative forcing model intercomparison project (RFMIP): experimental protocol for CMIP6. *Geosci. Model Dev.* **9**, 3447–3460 (2016).
50. Tsutsui, J. Diagnosing transient response to CO2 forcing in coupled atmosphere-ocean model experiments using a climate model emulator. *Geophys. Res. Lett.* **47**, e2019GL085844 (2020).
51. Tian, H. et al. A comprehensive quantification of global nitrous oxide sources and sinks. *Nature* **586**, 248–256 (2020).
52. Ganesan, A. L. et al. Advancing scientific understanding of the global methane budget in support of the Paris Agreement. *Glob. Biogeochem. Cycles* **33**, 1475–1512 (2019).
53. Held, I. M. et al. Probing the fast and slow components of global warming by returning abruptly to preindustrial forcing. *J. Clim.* **23**, 2418–2427 (2010).
54. Smith, M. A., Cain, M. & Allen, M. R. Further improvement of warming-equivalent emissions calculation. *Npj Clim. Atmos. Sci.* **4**, 1–3 (2021).
55. Hegerl, G. C. et al. Detecting greenhouse-gas-induced climate change with an optimal fingerprint method. *J. Clim.* **9**, 2281–2306 (1996).
56. Hasselmann, K. Multi-pattern fingerprint method for detection and attribution of climate change. *Clim. Dyn.* **13**, 601–611 (1997).
57. Morice, C. P. et al. An updated assessment of near-surface temperature change from 1850: the HadCRUT5 data set. *J. Geophys. Res. Atmos.* **126**, e2019JD032361 (2021).
58. Smith, T. M., Reynolds, R. W., Peterson, T. C. & Lawrimore, J. Improvements to NOAA's historical merged land–ocean surface temperature analysis (1880–2006). *J. Clim.* **21**, 2283–2296 (2008).
59. Rohde, R. A. & Hausfather, Z. The Berkeley Earth land/ocean temperature record. *Earth Syst. Sci. Data* **12**, 3469–3479 (2020).
60. Lenssen, N. J. L. et al. Improvements in the GISTEMP uncertainty model. *J. Geophys. Res. Atmospheres* **124**, 6307–6326 (2019).
61. Eyring, V. et al. Overview of the coupled model intercomparison project phase 6 (CMIP6) experimental design and organization. *Geosci. Model Dev.* **9**, 1937–1958 (2016).
62. Otto, A. et al. Energy budget constraints on climate response. *Nat. Geosci.* **6**, 415–416 (2013).
63. Stevens, B. Rethinking the lower bound on aerosol radiative forcing. *J. Clim.* **28**, 4794–4819 (2015).

ACKNOWLEDGEMENTS

S.J., M.R.A., T.W. and P.F. acknowledge funding from the European Union's Horizon 2020 research and innovation programme under grant agreement No 821003 (4 C project). S.J. is supported by the NERC Doctoral Training Partnership NE/L002612/1. The authors thank Chris Smith for contributing transient ERF time series calculated as part of RFMIP experiments for use in the production of Fig. 4 and Spencer Lindicoat for providing CMIP6 historical CO_2 emissions time series in Fig. 4.

AUTHOR CONTRIBUTIONS

S.J. and M.R.A. designed the study. M.C. and S.J. designed the simple formula approximating CO_2-fe emissions in Methods. P.F. contributed CMIP6 model diagnosed CO_2 emissions and temperatures from 1%/yr runs for TCRE estimates and NG provided CMIP6 GSAT and GMST time series for comparisons of budgets in Fig. 3. T.W. and S.J. completed analysis of CMIP6 historical runs to estimate GCM TCREs in Fig. 4. All authors contributed to writing.

COMPETING INTERESTS

The authors declare no competing interests.

ADDITIONAL INFORMATION

Supplementary information The online version contains supplementary material available at https://doi.org/10.1038/s41612-021-00203-9.

Correspondence and requests for materials should be addressed to Stuart Jenkins.

Reprints and permission information is available at http://www.nature.com/reprints

Publisher's note Springer Nature remains neutral with regard to jurisdictional claims in published maps and institutional affiliations.